

Dear Editor,

We thank you for your constructive criticism and comments. We acknowledge that comparing PET with the other drought indicators is not giving an additional value to the manuscript.

According that we've revised the paper by excluding all the comparison with PET. In order to do that we've changed the text accordingly (highlighted with track changes) and figures 5, 7 and 8 were modified.

Best regards,

Gustavo Naumann.

1 Comparison of drought indicators derived from multiple 2 datasets over Africa

3 **Gustavo Naumann¹, Emanuel Dutra², Paulo Barbosa¹, Florian Pappenberger²,**
4 **Fredrik Wetterhall² and Jürgen Vogt¹.**

5 [1]{European Commission, Joint Research Centre, Ispra, Italy }

6 [2]{European Centre for Medium Range Weather Forecasts, Reading, United Kingdom }

7 Correspondence to: G. Naumann (gustavo.naumann@jrc.ec.europa.eu)

8 9 **Abstract**

10 Drought monitoring is a key component to mitigate impacts of droughts. Lack of reliable and
11 up-to-date precipitation datasets is a common challenge across the Globe. This study
12 investigates different datasets and drought indicators on their capability to improve drought
13 monitoring in Africa. The study was performed for four river basins located in different
14 climatic regions (the Oum er-Rbia in Morocco, the Blue Nile in Eastern Africa, the Upper
15 Niger in Western Africa, and the Limpopo in South-Eastern Africa) as well as the Greater
16 Horn of Africa.

17 The five precipitation datasets compared are the *ECMWF ERA – Interim reanalysis*, the
18 *Tropical Rainfall Measuring Mission* satellite monthly rainfall product 3B-43, the *Global*
19 *Precipitation Climatology Centre* gridded precipitation dataset, the *Global Precipitation*
20 *Climatology Project* Global Monthly Merged Precipitation Analyses, and the *Climate*
21 *Prediction Center Merged Analysis of Precipitation*. The set of drought indicators used
22 includes the Standardized Precipitation Index, the Standardized Precipitation-Evaporation
23 Index, and Soil Moisture Anomalies. ~~Potential Evapotranspiration was also compared with~~
24 ~~the different drought indicators since it's a key process in the water cycle that can influence~~
25 ~~drought conditions.~~

26 A comparison of the annual cycle and monthly precipitation time series shows a good
27 agreement in the timing of the rainy seasons. The main differences between the datasets are in
28 the ability to represent the magnitude of the wet seasons and extremes. Moreover, for the
29 areas affected by drought, all the drought indicators agree on the time of drought onset and

1 recovery although there is disagreement on the extent of the affected area. In regions with
2 limited rain gauge data the estimation of the different drought indicators is characterised by a
3 higher uncertainty. Further comparison suggests that the main source of differences in the
4 computation of the drought indicators is the uncertainty in the precipitation datasets rather
5 than the estimation of the distribution parameters of the drought indicators.

6

7 **1 Introduction**

8 Assessment of drought impacts requires understanding of regional historical droughts as well
9 as the behaviours on human activities during their occurrences. Traditional methods for
10 drought assessment are mainly based on water supply indices derived from precipitation time-
11 series alone (Heim 2002). A sparse distribution of rain gauges and short or incomplete
12 historical rainfall records may, however, lead to significant errors in the estimation of water
13 supply indices derived from precipitation time-series.

14 As a consequence of drought, many countries in Africa have seen recurrent famines that
15 affected millions of people (Rojas et al., 2011). Since precipitation is fundamental for rain-fed
16 crops in these drought-prone regions, improvements in drought monitoring and early warning
17 will improve our capacity to detect, anticipate, and mitigate famine (Wilhite et al, 2000,
18 Rowland et al., 2005). However, the lack of reliable and up-to-date climatological data in
19 many regions of Africa hinders the development of effective real-time drought monitoring
20 and early warning systems.

21 Recently, several rain gauge and remote sensing based estimations of precipitation became
22 available, which exhibit discrepancies and limitations in representing rainfall at local and
23 regional scale. This has been highlighted for daily and monthly precipitation datasets by
24 Dinku et al (2007; 2008) and Hirpa et al (2010). The authors studied a relatively dense station
25 network over the Ethiopian highlands and found that at a monthly time scale and a spatial
26 resolution of 2.5° CMAP and TRMM 3B-43 performed very well with a bias of less than 10%
27 and a root mean square error of about 25%. Thiemig et al. (2012; 2013) found that the
28 Rainfall Estimation Algorithm and TRMM 3B-42 showed a high potential in reproducing the
29 interannual variability, the spatial and quantitative distribution and the timing of rainfall
30 events.

1 Liebmann et al., 2012, studied the spatial variations in the annual cycle comparing GPCP with
2 TRMM and gauge-based Famine Early Warning System datasets. They found that GPCP
3 estimates are generally higher than TRMM in the wettest parts of Africa, but the timing of the
4 annual cycle and onset dates are consistent. Dutra et al., 2013a, found significant differences
5 (mainly in the equatorial area) in the quality of the precipitation between the ERA-Interim,
6 GPCP and the Climate Anomaly Monitoring System – Outgoing Longwave Radiation
7 Precipitation Index (CAMS-OPI) datasets for different river basins in Africa. From these
8 studies it is evident that the question on which dataset best represents African precipitation is
9 still not sufficiently answered.

10 The difficulty in establishing a “ground truth” of precipitation in Africa also affects the
11 uncertainty in the calculation of derivatives of precipitation, like drought indicators, since the
12 relationship between the quality of a precipitation product and any drought indicator is
13 nonlinear. This means that errors in the precipitation can be amplified or dampened when a
14 drought index is computed. Previous works have reviewed and compared several drought
15 indicators (Heim 2002; Anderson et al 2011, Shukla et al 2011; Vicente-Serrano et al 2012).
16 However, an agreement between different indicators is not necessarily observed as the
17 capability to detect droughts changes between indicator, system and region.

18 The main goal of this study was to identify the main sources of uncertainty in the computation
19 of the drought indicators. Furthermore, an assessment was done on the ability of the different
20 datasets and drought indicators (SPI, SPEI, ~~PET~~ and SMA) to represent the spatio-temporal
21 features of droughts in different climate regimes across Africa.

22

23 **2 Data and Methods**

24 **2.1 Study area**

25 The analysis was performed at continental level over Africa with particular focus on the areas
26 falling in four river basins (Oum er-Rbia, Limpopo, Niger, and Eastern Nile) as well as the
27 Greater Horn of Africa (GHA). The regions were defined as the land areas inside each
28 bounding box (see Figure 1). The area and geographical extent of the study areas are provided
29 in Table 1. The regional study areas selected cover a range of climates and socio-economic
30 systems in Africa.

1

2 **2.2 Precipitation Data**

3 The five precipitation datasets used were the ECMWF ERA-INTERIM (ERA-I) Reanalysis
4 (approximately $0.7^{\circ} \times 0.7^{\circ}$, bilinear interpolation to $0.5^{\circ} \times 0.5^{\circ}$), Tropical Rainfall Measuring
5 Mission (TRMM) satellite monthly rainfall product 3B-43 ($0.25^{\circ} \times 0.25^{\circ}$), the Global
6 Precipitation Climatology Centre (GPCC) gridded precipitation dataset V.5 ($0.5^{\circ} \times 0.5^{\circ}$), the
7 Global Precipitation Climatology Project (GPCP) Global Monthly Merged Precipitation
8 Analyses ($2.5^{\circ} \times 2.5^{\circ}$) and the CPC Merged Analysis of Precipitation (CMAP, $2.5^{\circ} \times 2.5^{\circ}$)
9 (Table 2).

10 This work uses the TRMM Multisatellite Precipitation Analysis estimation computed at
11 monthly intervals as TRMM 3B-43 dataset for the period 1998-2010 (Huffman et al., 2007).
12 This product combines the estimates generated by the TRMM and other satellite products
13 (3B-42) with the Climate Anomaly Monitoring System gridded rain gauge data and/or the
14 GPCC global rain gauge data at $0.25^{\circ} \times 0.25^{\circ}$ resolution. The GPCC full reanalysis version 5
15 (Rudolf et al., 1994) was used for 1979 to 2010. This dataset is based on quality-controlled
16 precipitation observations from a large number of stations (up to 43,000 globally) with
17 irregular coverage in time.

18 The ECMWF ERA-I reanalysis, the latest global atmospheric reanalysis produced by
19 ECMWF extends from 1 January 1979 to the present date. See Dee et al. (2011) for detailed
20 descriptions of the atmospheric model used in ERA-I, the data assimilation system, the
21 observations used, and various performance aspects. The ERA-I configuration has a spectral
22 T255 horizontal resolution (about $0.7^{\circ} \times 0.7^{\circ}$ in the grid-point space) with 60 model vertical
23 levels. For the present application, the monthly precipitation means were spatially
24 interpolated (bilinear) to a regular $0.5^{\circ} \times 0.5^{\circ}$ grid. Three-hourly ERA-I precipitation estimates
25 are produced by 12 h model integrations starting at 00UTC and 12UTC. These short-range
26 forecasts are therefore mainly constrained by the analysis of upper-air observations of
27 temperature and humidity, from satellites and in situ instruments.

28 The Global Precipitation Climatology Project (GPCP, Huffman et al., 2009) combines the
29 precipitation information available from several sources such as the Special Sensor
30 Microwave/Imager (SSM/I) data from the United States Defence Meteorological Satellite

1 Program satellites, infrared precipitation estimates computed primarily from geostationary
2 satellites, low-Earth orbit estimates including the Atmospheric Infrared Sounder Television
3 Infrared Observation Satellite Program (TIROS) Operational Vertical Sounder (TOVS), and
4 Outgoing Longwave Radiation Precipitation Index data from the NOAA series satellites. The
5 gauge data included are assembled and analyzed by the Global Precipitation Climatology
6 Centre (GPCC). The latest version of GPCP v2.2 that was used is available since January
7 1979 to December 2010 in a regular 2.5°x2.5° grid.

8 The CPC Merged Analysis of Precipitation ("CMAP") is a technique which produces pentad
9 and monthly analyses of global precipitation in which observations from rain gauges are
10 merged with precipitation estimates from several satellite-based sensors (infrared and
11 microwave). The analysis are on a 2.5 x 2.5 degree latitude/longitude grid and extend back to
12 1979. For further information refer to Xie and Arkin, (1997).

13 **2.3 Drought indicators**

14 The set of hydro-meteorological indicators analysed included the Standardized
15 Precipitation Index (SPI), Standardized Precipitation-Evaporation Index (SPEI), and Soil
16 Moisture Anomalies (SMA). ~~A discussion on the possible relation of Potential
17 Evapotranspiration (PET) with the different indicators is also presented. Even if
18 EvaporationPET is not a drought indicator itself, it is one of the key processes in the water
19 cycle and usually gives a more complete accounting of drought variability and that can help to
20 understand differences in drought indicators. However, the estimation of continental
21 evapotranspiration fluxes is complex and can be a source of uncertainties when assessing
22 drought conditions (Trambauer et al., 2014).~~ The SPI was computed with all the datasets
23 (ERA-I, TRMM, and GPCP) since it only uses precipitation data. The SPEI was computed
24 with precipitation and potential evapotranspiration from ERA-I, as well as with precipitation
25 from GPCP and potential evapotranspiration from ERA-I. SMA and PET were directly
26 obtained from the ERA-I reanalysis. The individual drought episodes from the time series of
27 all indicators were determined by considering different thresholds of the standardized
28 indicators. The duration of each dry event was determined as the number of consecutive
29 months with negative values of the drought indices (~~positive for PET~~) over the period 1998-
30 2010. The monthly drought fractional area was computed for different thresholds but is only
31 shown for the values below the -1.0 threshold.

2.3.1 Standardized Precipitation Index (SPI)

The Standardized Precipitation Index (SPI) was developed by McKee et al. (1993, 1995) to provide a spatially and temporally invariant measure of the precipitation deficit (or surplus) for any accumulation timescale (e.g. 3, 6, 12 months). It is computed by fitting a parametric Cumulative Distribution Function (CDF) to a homogenized precipitation time-series and applying an equi-probability transformation to the standard normal variable. This gives the SPI in units of number of standard deviations from the median.

Typically, the gamma distribution is the parametric CDF chosen to represent the precipitation time-series (e.g. McKee et al., 1993, 1995; Lloyd-Hughes and Saunders 2002; Husak et al., 2007) since it has the advantage of being bounded on the left at zero and positively skewed (Thom 1958; Wilks 2002). Moreover, Husak et al. (2007) and Naumann et al. (2012) have shown that the gamma distribution adequately models precipitation time-series in most of the locations over Africa. In this study we use the Maximum-Likelihood Estimation (MLE) method to estimate the parameters of the gamma distribution.

A persistent negative anomaly of precipitation is the primary driver of drought, resulting in a successive shortage of water for different natural and human needs. Since SPI values are given in units of standard deviation from the standardised mean, negative values correspond to drier periods than normal and positive values correspond to wetter periods than normal. The magnitude of the departure from the median is a probabilistic measure of the severity of a wet or dry event.

~~2.3.2 Standardized Precipitation-Evaporation Index (SPEI) and Potential Evapotranspiration (PET)~~

The Standardized Precipitation Evapotranspiration Index (SPEI, Vicente-Serrano et al., 2010) is based on precipitation and temperature data, and it has the advantage of combining different time dimensions (like the SPI) with the capacity to include the effects of temperature variability on drought. The calculation combines a climatic water balance, the accumulation of a water deficit/surplus at different time scales, and an adjustment to a log-logistic probability distribution. SPEI is similar to SPI, but it includes the temperature impact via the potential evapotranspiration (PET) that is calculated following Thornthwaite (1948). In the current work, we used ERA-I 2-meter temperature to derive PET, and the multiscalar index is

1 calculated as P-PET over the different time-scales and normalized (like the SPI) using the log-
2 logistic probability distribution.

3 2.3.32.3.2 **Soil Moisture Anomalies (SMA)**

4 Soil moisture anomalies were derived from ERA-I simulations by removing the mean annual
5 cycle. Further standardization could be achieved by fitting the soil moisture distribution to a
6 probability distribution (similar to SPI or, SPEI) such as the Beta distribution (Sheffield et al.,
7 2004) or just a simple z-score (Dutra et al., 2008). In the current work we compare the SMA
8 z-score following the considerations depicted in Dutra et al., 2008. By normalizing the soil
9 moisture with the z-score, a classification scheme is obtained that is similar and comparable to
10 that of McKee et al. (1993) and Vicente Serrano et al. (2012).

11 **2.4 Evaluation metrics**

12 The precipitation datasets and drought indicators were assessed using different scores
13 available in the hydroGOF R-Package (Zambrano-Bigarini, 2013): Spearman's correlation
14 coefficient (r), Mean Absolute Difference (MAD), Percent Bias (PBIAS) between two
15 products and the Index of Agreement (d). Details of the Evaluation scores are listed in the
16 appendix.

17 A direct quantitative assessment at continental level is difficult due to the lack of an actual
18 validation dataset that represents the ground truth with adequately high spatial or temporal
19 resolution. The performance metrics (mean absolute difference, relative bias and index of
20 agreement) were used to diagnose the relative reliability of each indicator over different
21 drought properties. This analysis does not assume that a single dataset or indicator is better
22 than the other but highlights their temporal and spatial coherency.

24 **3 Results and discussion**

25 **3.1 Comparison of global precipitation datasets**

26 The datasets analysed are based on in-situ data (GPCC), remote sensing estimations (TRMM,
27 GPCP) and a global circulation model (ERA-I). The datasets are not completely independent.
28 For example, TRMM and GPCP are mainly based on remote sensing data and GPCP uses

1 GPCC over land). Figure 2 shows the mean annual precipitation for the ERA-I, GPCC,
2 GPCP, CMAP and TRMM datasets over Africa. There is an overall agreement between the
3 datasets with respect to the mean as well as the general spatial patterns of annual
4 precipitation. These datasets agree on the north-south gradient from the Sahara desert areas in
5 the North to the tropical savannahs in the Sahel (an area centered at approximately 10°N
6 spanning from the Atlantic Ocean in the west to the Red Sea in the east). The datasets also
7 agree in the areas of maximum precipitation over the African rainforests related to the
8 location of the Inter-tropical Convergence Zone (ITCZ), as well as in the drier climate of the
9 south-western part of Africa. The main differences are observed in the tropical area and over
10 un-gauged areas. In transition regions from the Sahel to the Sahara TRMM estimations can
11 exceed GPCC more than twofold while TRMM is substantially lower than the other
12 estimations along the southwestern coast of West Africa (Liebmann et al., 2012). There is
13 also a tendency of higher precipitation in the tropical rainforest in GPCP (Liebmann et al.,
14 2012) and ERA-I (Dutra et al., 2013a, b) compared with the other datasets. ERA-I
15 overestimates the rainfall in the central African region which is likely to be associated with a
16 substantial warm bias in the model due to an underestimation of aerosol optical depth in the
17 region (Dee et al., 2011).

18 For all the datasets and regions analysed the mean annual cycle of precipitation shows good
19 agreement with respect to the onset and end of the rainy season. This is true even for the GHA
20 region which is characterized by two rainy seasons (Figure 3). However, with respect to
21 intensity the results are more heterogeneous. Although in the Limpopo and Oum er-Rbia
22 basins there is a good agreement between the datasets, for the basins located in the tropical
23 band the discrepancies are higher with an overestimation of ERA-I in the Eastern Nile Basin
24 and GHA and an underestimation in the Niger basin.

25 Apparently the density of rain gauges plays a role in determining the agreement between
26 datasets. The best gauged regions (Oum er-Rbia and Limpopo; Table 1) are those with the
27 lowest dispersion in terms of annual cycle. These two regions (Oum er-Rbia and Limpopo)
28 are located outside the tropical region, and their precipitation variability is mainly controlled
29 by large-scale synoptic weather systems, while in the tropical region small-scale convective
30 events play an important role. In these regions, model uncertainties (for example land-
31 atmosphere coupling), uncertainties in satellite retrievals as well as poor gauge cover
32 contribute to the large spread in the mean annual cycles computed with the different datasets.

1 The monthly datasets show a reasonable agreement over all regions in terms of the correlation
2 coefficients which are usually greater than 0.8 (Table 3). The CMAP dataset deviates with
3 values below 0.7 in some regions. Oum er-Rbia and Limpopo areas show the best agreement
4 between datasets with MAE values below 10 mm/month. The bias in those two regions is
5 below 20 % in all the cases except when TRMM and CMAP are compared (30%).

6 The biggest differences were observed for ERA-I in the Blue Nile and GHA regions. In these
7 regions the overestimation of monthly precipitation reached 40 mm/month and the bias can
8 reach 90% in the Blue Nile and around 50% in the GHA. These discrepancies are mainly due
9 to the problems of representation of the mean annual cycle of precipitation by atmospheric
10 models and the lack of in-situ observations (Mariotti et al., 2011, Dutra et al., 2013b).

11 **3.2 Comparison of drought indicators**

12 The monthly patterns of drought over Africa for January 2000, 2003, 2006 and 2009 show
13 that dry areas (indicators with negative values) are generally depicted in more than one
14 indicator, but their consistency varies with the drought characteristics, as well as the spatial
15 and temporal coverage (Figure 4). Although there is in general a good spatial correspondence
16 between all the indicators over the study period, there are also areas where there is no
17 agreement between some indicators, such as in Central Africa between SPI and SPEI.

18 Figure 5 shows the index of agreement (d) between all the drought indicators computed with
19 ERA-I. Overall, the index of agreement shows that there is a good correspondence between
20 indicators in all regions with mean d values greater than 0.5 for almost all the comparisons.

21 ~~PET seems to be uncoupled with the other indicators with showing low values of d. Maybe~~
22 ~~using different PET products could improve the index of agreement, since This may reflect~~
23 ~~the high disparities between different PET products that still is observed in the continent have~~
24 ~~been reported for Africa (Trambauer et al., 2014).~~ However, the effect on the computations of
25 the SPEI is not major, since the agreement of this indicator with the others is still high. Only
26 the inner Niger Delta is characterized by a weaker agreement, where d is often below 0.5.

27 Figure 6 shows the evolution of drought areas in 2000, 2003, 2006 and 2009 characterized by
28 the number of indicators below a certain threshold. In almost all areas there is a good
29 agreement, with usually more than 3 indicators reporting drought conditions per grid cell.
30 However, there are some areas with only one indicator below the defined threshold, mostly

1 over Central Africa. There is scope to take advantage of these discrepancies and agreements
2 and propose the construction of a composite indicator (Svoboda et al., 2002; Sepulcre-Canto
3 et al., 2012; Hao and AghaKouchak, 2013). The development of a single composite drought
4 indicator could improve the detection of the onset of a drought and help to monitor its
5 evolution more efficiently, at the same time providing information on the uncertainty in the
6 data. This will allow decision makers and stakeholders to better handle uncertainties in early
7 warning systems.

8 The individual drought episodes were computed from the time series of all indicators
9 considering as dry periods all values of standardized indicators below zero. The duration of
10 each dry event was determined as the number of consecutive months with negative values
11 ~~(positive for PET)~~ for the period 1998-2010. The average duration of dry episodes lasted
12 between 2 to 6 months for all indicators, with the largest differences in duration for different
13 indicators being found in the Niger basin and in the GHA (Figure 7). Overall, dry periods
14 measured with SPEI tend to be 1 or 2 months more persistent if compared with the other
15 estimations, ~~while PET is the variable with less memory.~~

16 Figure 8 shows the monthly fractional area under standardised values below -1.0. For the
17 areas that are under drought, all the datasets agree with the time of onset and recovery but
18 there are sometimes disagreements on the area affected and this disagreement tends to be
19 dependent on the threshold selected. In general there is a better agreement if the areas covered
20 by any standardised indicator below -1.0 are considered. In this analysis the Niger basin and
21 Greater Horn of Africa present more discrepancies reaching a difference of more than 50%
22 between SPI and SPEI estimations during the 2009/2010 and 2005/2006 periods respectively.
23 The soil moisture anomalies tend to define less generalised droughts as it is hard to reach half
24 the region under dry conditions. However, even if the magnitude of the area is smaller with
25 respect to the other indicators, the soil moisture shows a good correspondence except for the
26 period 2000/2002 in the inner Niger delta.

27 In order to define how the selected threshold could affect the agreement between datasets a
28 correlation analysis was performed between different thresholds of SPI and the areas affected
29 by droughts in each region. Here the results of the different SPI estimations are presented,
30 however similar results were found for the other indicators (not shown). For almost all
31 regions (except for Oum er-Rbia where this relationship is almost constant) the correlation

1 between the different SPI's is higher for thresholds closer to zero (Figure 9). To consider a
2 higher threshold (i.e. less negative) to define areas affected by drought (e.g. -0.8 or -1),
3 therefore, will reduce the disagreement between indicators. However it puts a limit to the
4 detection of the significance and severity of a drought. These results highlight that the main
5 differences between the indicators appear in the extreme events.

6 Also, the bias between estimations indicates an acceptable departure between estimations
7 from normal conditions until values near -0.5 (Figure 10). Below this threshold the bias
8 increases exponentially surpassing quickly a bias of 100% around SPI values of -1. For Niger
9 and GHA regions there is only a reasonable agreement between ERA-I and GPCC
10 estimations.

11 Generally in the Oum er-Rbia and Limpopo basins, both extra-tropical regions, the agreement
12 is high, possibly due to the greater number of in-situ observations and the importance of
13 large- scale synoptic weather systems in these areas.

14 For the basins located between the tropics a greater disagreement is observed due to different
15 factors. The main common factor is the remarkable absence of observations to calibrate and
16 test the datasets. These deficiencies are also more evident in complex mountainous areas such
17 as the Eastern Nile basin. Furthermore, droughts in equatorial regions are mainly driven by
18 the absence of convective events during the rainy season. These mesoscale dimension events
19 are hard to be reproduced by models and even difficult to monitor in areas with scarce in-situ
20 rain gauges.

21 For drier regions, such as the inner Niger delta and the GHA, the estimation of the distribution
22 parameters needed for the computation of the standardized indicators can be biased (or lower
23 bounded) by the large amount of zero or near null precipitation observations. As depicted in
24 Wu et al. (2007), the estimation of the gamma probability density function and the limited
25 sample size in dry areas reduce the confidence of the SPI values. In these cases, the SPI may
26 never attain the necessary threshold and hence failing to detect some drought occurrences
27 (e.g. SPI always above -1 in Niger and GHA). The discrepancies between indicators for lower
28 thresholds over regions with limited rain gauge data is characterised by the uncertainties of
29 extreme values. This suggests that the main sources of error are the uncertainties in the
30 precipitation datasets that are propagated in the estimation of the distribution parameters of
31 the drought indicators.

1 The above discussion underlines the fact that drought monitoring and assessment is a difficult
2 task, not only due to the nature of the phenomenon, but also due to the limitations inherent in
3 the availability of long-term and high quality datasets for extended regions. The
4 meteorological datasets as well as the indicators and models used must be selected carefully
5 and their limitations need to be taken into account. As a consequence no definite conclusion
6 can be drawn for the use of a single dataset or indicator. Depending on the region to be
7 studied, different combinations may have to be chosen.

8 Our results further underline the value of maintaining an operational monitoring network at
9 country, continental or even global level since indirect observations have their intrinsic
10 uncertainties linked to the availability and reliability of ‘ground truth’ for their calibration.
11 Without proper calibration, model (ERA-I) or algorithm (TRMM) inherent errors can
12 propagate resulting in large drought indicator uncertainties, bringing no added value with
13 respect to using standard climatology.

14 The development of a combined indicator based on a probabilistic approach (e.g., Dutra et al.,
15 2013c) could be useful as a monitoring product at continental level. However, at local scale
16 the kind of indicator and the source of data must be chosen carefully taking into account their
17 limitations.

18

19 **4 Conclusions**

20 This study evaluated the capabilities of different drought indicators, ~~(including SPI, SPEI, and~~
21 ~~SMA, as well as PET estimations and SMA),~~ in detecting the timing and extension of drought
22 across Africa, using five different precipitation datasets (TRMM, ERA-Interim, GPCC, GPCP
23 and CMAP). The analysis was performed on a Pan-African scale and on a regional scale
24 focused on four river basins and on the Greater Horn of Africa.

25 A comparison of the annual cycle and monthly precipitation time series shows a good
26 agreement in the timing of the peaks, including the Greater Horn of Africa where there are
27 two rainy seasons. The main differences are observed in the ability to represent the
28 magnitude of the wet seasons.

29 The monthly mean precipitation datasets shows good agreement over all regions with the only
30 exception of the CMAP dataset that shows a lower agreement. In the Oum er-Rbia and

1 Limpopo basins there is a good agreement between the datasets with mean absolute
2 differences below 10 mm/month. The bias in those two regions is below 20 %. The worst
3 performance of ERA-I was observed in the Blue Nile basin, overestimating the monthly
4 precipitation up to 40 mm/month with a bias of up to 92% with respect to the other datasets.
5 Also in the GHA region the bias is around 50% with an overestimation of up to 17
6 mm/month.

7 The comparative analysis between TRMM, ERA-I, GPCP and GPCC datasets suggests that it
8 is feasible to use TRMM time series with high spatial resolution for reliable drought
9 monitoring over parts of Africa. It is possible to take advantage of this dataset mainly at
10 regional level due to its high spatial resolution. However, higher discrepancies in SPI
11 estimations are shown in mountainous areas and areas with a sparse in situ station density.
12 On the other hand, drought monitoring at continental level with ERA-I performs better
13 outside the areas influenced by the ITCZ.

14 The comparison between drought indicators suggests that the main discrepancies are due to
15 the uncertainties in the datasets (driven by a lack of ground information, uncertainties in the
16 estimation algorithms or the parameterization of the convection) rather than to the estimation
17 of the distribution parameters. This is why the SPI estimations for the Oum er-Rbia and
18 Limpopo regions exhibit a better agreement between estimations. While for the other regions
19 the discrepancies between datasets are in many cases acceptable, greater discrepancies are
20 observed for the inner Niger Delta when comparing ERA-I estimations with the other
21 datasets.

22 Regarding the areas that are under drought, all the indicators agree with the time of onset and
23 recovery but there are sometimes disagreements with respect to the area affected, and the
24 level of disagreement tends to be dependent on the threshold selected.

25 It is proposed to integrate different indicators and accumulation periods in the form of a
26 multivariate combined indicator in order to take advantage of their different drought
27 properties. The probabilistic nature of such an approach would be very helpful for decision
28 makers and for the combined analysis of multiple risks.

29

30 **Acknowledgements**

1 This work was funded by the European Commission Seventh Framework Programme (EU
2 FP7) in the framework of the Improved Drought Early Warning and Forecasting to Strengthen
3 Preparedness and Adaptation to Droughts in Africa (DEWFORA) project under Grant
4 Agreement 265454. Gustavo Naumann thanks Mauricio Zambrano-Bigarini for the important
5 discussions about different metrics to compare indicators and to make available the
6 hydroGOF R-package.

7

1 **Appendix A**

2 The Spearman correlation represents the Pearson correlation coefficient computed using the
3 ranks of the data. Conceptually, the Pearson correlation coefficient is applied to the ranks of
4 the data rather than to the data values themselves. The Spearman coefficient is a more robust
5 and resistant alternative to the Pearson product-moment correlation coefficient (Wilks, 2002).
6 Computation of the Spearman rank correlation can be described as:

$$7 \quad r = 1 - \frac{6 \sum R_i^2}{n(n^2 - 1)} \quad (1)$$

8 where R_i is the difference in ranks between the i th pair of data values. In cases of ties, where a
9 particular data value appears more than once, all of these equal values are assigned their
10 average rank before computing the R_i 's.

11 The Mean Absolute Difference (MAD) measures the average magnitude of the differences in
12 a set of different estimations of a certain indicator. It measures accuracy for continuous
13 variables without considering the direction of the error. Also, this quantity is usually used to
14 measure how close are two datasets or indicators as shown in equation 2

$$15 \quad MAD = \frac{1}{n} \sum_{i=1}^n |X1_i - X2_i| \quad (2)$$

16 where $X1$ and X are the values of precipitation or drought indicator of dataset 1 and n
17 represents the number of pairs The percent bias (PBIAS) measures the average tendency of
18 the values of a certain dataset to be larger or smaller than a reference one.

$$19 \quad PBIAS = 100 \frac{\sum_{i=1}^n (X1_i - X2_i)}{\sum_{i=1}^n X1_i} \quad (3)$$

20 The optimal value of PBIAS is 0, with low-magnitude values indicating accurate
21 representation of drought indicators. Positive values indicate an overestimation bias, whereas
22 negative values indicate an underestimation bias. It must be taken into account that this metric
23 depends on which dataset is considered to represent the observations.

24 The Index of Agreement (d) developed by Willmott (1981) as a standardized measure of the
25 degree of model prediction error varies between 0 and 1. A value of 1 indicates a perfect
26 match, and 0 indicates no agreement at all (Willmott, 1981). The index of agreement can

1 detect additive and proportional differences in the observed and simulated means and
2 variances; however, it is overly sensitive to extreme values due to the squared differences
3 (Legates and McCabe, 1999).

$$4 \quad d = 1 - \frac{\sum(x_1 - x_2)^2}{\sum(|x_2 - \bar{x}_1| + |x_1 - \bar{x}_1|)} \quad (4)$$

5

1 **References**

- 2 Anderson, M. C., Hain, C., Wardlow, B., Pimstein, A., Mecikalski, J. R., and Kustas, W. P.:
3 Evaluation of drought indices based on thermal remote sensing of evapotranspiration over the
4 continental United States. *Journal of Climate*, 24(8), 2025-2044, 2011.
- 5 Dee, D., and Coauthors: The ERA-Interim reanalysis: Configuration and performance of the
6 data assimilation system. *Quart. J. Roy. Meteor. Soc.*, 137, 553–597, 2011.
- 7 Dinku, T., Ceccato, P., Grover-Kopec, E., Lemma, M., Connor, S. J., and Ropelewski, C. F.:
8 Validation of satellite rainfall products over East Africa's complex topography. *International*
9 *Journal of Remote Sensing*, 28(7), 1503-1526, 2007.
- 10 Dinku, T., Chidzambwa, S., Ceccato, P., Connor, S. J., & Ropelewski, C. F.: Validation of
11 high-resolution satellite rainfall products over complex terrain. *International Journal of*
12 *Remote Sensing*, 29(14), 4097-4110, 2008.
- 13 Dutra, E., Viterbo, P., and Miranda, P. M. A.: ERA-40 reanalysis hydrological applications in
14 the characterization of regional drought, *Geophys. Res. Lett.*, 35, L19402,
15 doi:19410.11029/12008GL035381, 2008.
- 16 Dutra, E., Giuseppe, F. D., Wetterhall, F., & Pappenberger, F.: Seasonal forecasts of droughts
17 in African basins using the Standardized Precipitation Index. *Hydrology and Earth System*
18 *Sciences*, 17(6), 2359-2373, 2013a.
- 19 Dutra, E., Magnusson, L., Wetterhall, F., Cloke, H. L., Balsamo, G., Boussetta, S., &
20 Pappenberger, F.: The 2010–2011 drought in the Horn of Africa in ECMWF reanalysis and
21 seasonal forecast products. *International Journal of Climatology*, 33, 7, 1720–1729, 2013b.
- 22 Dutra, E., Wetterhall, F., Di Giuseppe, F., Naumann, G., Barbosa, P., Vogt J., Pozzi W., and
23 Pappenberger F.: Global meteorological drought: Part I - probabilistic monitoring, to be
24 submitted to HESS, 2013c.
- 25 Hao, Z., & AghaKouchak, A.: Multivariate Standardized Drought Index: A parametric multi-
26 index model. *Advances in Water Resources*, 57, 12-18, 2013.
- 27 Heim Jr, R. R.: A review of twentieth-century drought indices used in the United States.
28 *Bulletin of the American Meteorological Society*, 83(8), 1149-1165, 2002.

1 Hirpa, F. A., Gebremichael, M., and Hopson, T.: Evaluation of high-resolution satellite
2 precipitation products over very complex terrain in Ethiopia. *Journal of Applied Meteorology*
3 *and Climatology*, 49(5), 1044-1051, 2010.

4 Huffman and Coauthors: The TRMM Multi-satellite Precipitation Analysis (TMPA): Quasi-
5 global, multiyear, combined sensor precipitation estimates at fine scales. *J. Hydrometeor.*, 8,
6 38–55, 2007.

7 Huffman, G.J, R.F. Adler, D.T. Bolvin, and Gu G.: Improving the Global Precipitation
8 Record: GPCP Version 2.1. *Geophys. Res. Lett.*, 36,L17808, doi:10.1029/2009GL040000,
9 2009.

10 Husak, G. J., Michaelsen, J., and Funk, C.: Use of the gamma distribution to represent
11 monthly rainfall in Africa for drought monitoring applications. *International Journal of*
12 *Climatology*, 27(7), 935-944, 2007.

13 Legates, D. R., and McCabe Jr., G. J.: Evaluating the Use of "Goodness-of-Fit" Measures in
14 Hydrologic and Hydroclimatic Model Validation, *Water Resour. Res.*, 35(1), 233–241, 1999.

15 Liebmann, B., Bladé, I., Kiladis, G. N., Carvalho, L. M., B. Senay, G., Allured, D., Leroux,
16 S., and Funk, C.: Seasonality of African precipitation from 1996 to 2009. *Journal of Climate*,
17 25(12), 4304-4322, 2012.

18 Lloyd-Hughes, B., and Saunders, M. A.: A drought climatology for Europe. *Int. J. Climatol.*,
19 22, 1571–1592, 2002.

20 Mariotti, L., Coppola, E., Sylla, M. B., Giorgi, F., and Piani, C.: Regional climate model
21 simulation of projected 21st century climate change over an all-Africa domain: Comparison
22 analysis of nested and driving model results. *J. Geophys. Res.*, 116, D15111,
23 doi:10.1029/2010JD015068, 2011.

24 McKee T.B., Doesken N.J., and Kleist J.: The Relationship of Drought Frequency and
25 Duration to Time Scales. *Proc. 8th Conf. on Appl. Clim.*, 17-22 Jan. 1993, Anaheim, CA,
26 179-184, 1993.

27 McKee, T. B., Doesken, N. J., and Kleist, J.: Drought monitoring with multiple time scales.
28 *Proc. Ninth Conf. on Applied Climatology*, Dallas, TX, Amer. Meteor. Soc. 233-236, 1995.

1 Naumann, G., Barbosa, P., Carrao, H., Singleton, A., and Vogt, J.: Monitoring Drought
2 Conditions and Their Uncertainties in Africa Using TRMM Data. *Journal of Applied*
3 *Meteorology and Climatology*, 51(10), 1867-1874, 2012.

4 Rojas, O., Vrieling, A., and Rembold, F.: Assessing drought probability for agricultural areas
5 in Africa with coarse resolution remote sensing imagery. *Remote Sensing of Environment*
6 115.2, 343-352, 2011.

7 Rowland, J., Verdin, J., Adoum, A., and Senay, G.: Drought monitoring techniques for famine
8 early warning systems in Africa, in: *Monitoring and Predicting Agricultural Drought: A*
9 *Global Study*, edited by: Boken, V. K., Cracknell, A. P., and Heathcote, R. L., Oxford
10 University Press, New York, 252–265, 2005.

11 Rudolf, B., W. Rueth, and Schneider, U.: Terrestrial precipitation analysis: Operational
12 method and required density of point measurements. *Global Precipitation and Climate*
13 *Change*, M. Desbois and F. Desahmond, Eds., Springer-Verlag, 173–186, 1994.

14 Sepulcre-Canto, G., Horion, S., Singleton, A., Carrao, H., and Vogt, J.: Development of a
15 Combined Drought Indicator to detect agricultural drought in Europe. *Natural Hazards and*
16 *Earth System Science*, 12(11), 3519-3531, 2013.

17 Sheffield, J., Goteti, G., Wen, F. H., and Wood, E. F.: A simulated soil moisture based
18 drought analysis for the United States, *J. Geophys. Res.*, 109(D24), 2004.

19 Shukla, S., Steinemann, A. C., & Lettenmaier, D. P.: Drought monitoring for Washington
20 State: Indicators and applications. *Journal of Hydrometeorology*, 12(1), 66-83, 2011.

21 Svoboda, M. D., and Coauthors: The drought monitor. *Bull. Amer. Meteor. Soc.*, 83, 1181-
22 1189, 2002.

23 Thiemig, V., Rojas, R., Zambrano-Bigiarini, M., Levizzani, V., and De Roo, A.: Validation of
24 Satellite-Based Precipitation Products over Sparsely Gauged African River Basins. *Journal of*
25 *Hydrometeorology*, 13(6), 1760-1783, 2012.

26 Thiemig, V., Rojas, R., Zambrano-Bigiarini, M., and De Roo, A.: Hydrological Evaluation of
27 Satellite-Based Rainfall Estimates over the Volta and Baro-Akobo Basin. *Journal of*
28 *Hydrology*, 499, 324-338, 2013.

29 Thom, H. C.: A note on the gamma distribution. *Monthly Weather Review*, 86(4), 117-122,
30 1958.

1 Thornthwaite, C. W.: An approach toward a rational classification of climate. *Geogr. Rev.*,
2 38, 55–94, 1948.

3 ~~[Trambauer, P., Dutra, E., Maskey, S., Werner, M., Pappenberger, F., van Beek, L. P. H., and](#)~~
4 ~~[Uhlenbrook, S.: Comparison of different evaporation estimates over the African continent,](#)~~
5 ~~[Hydrol. Earth Syst. Sci., 18, 193–212, doi:10.5194/hess-18-193-2014, 2014.](#)~~

6 Vicente-Serrano, S. M., Beguería, S., and López-Moreno, J. I.: A multiscalar drought index
7 sensitive to global warming: the standardized precipitation evapotranspiration index. *Journal*
8 *of Climate*, 23(7), 1696–1718, 2010.

9 Vicente-Serrano, S. M., Beguería, S., Gimeno, L., Eklundh, L., Giuliani, G., Weston, D., El
10 Kenawy, A., López-Moreno, J., Nieto, R., Ayenew T., Konte, D., Ardö, J., and Pegram, G.
11 G.: Challenges for drought mitigation in Africa: The potential use of geospatial data and
12 drought information systems. *Applied Geography*, 34, 471–486, 2012.

13 Wilhite, D. A., and Svoboda, M., D.: "Drought early warning systems in the context of
14 drought preparedness and mitigation." *Early warning systems for drought preparedness and*
15 *drought management*, 1–21, 2000.

16 Wilks D.S.: *Statistical Methods in the Atmospheric Sciences*. Elsevier Academic Press
17 Publications, 467 pp., 2002.

18 Willmott, C. J.: On the validation of models. *Physical Geography*, 2, 184–194, 1981.

19 Wu, H., Svoboda, M. D., Hayes, M. J., Wilhite, D. A., and Wen, F.: Appropriate application
20 of the standardized precipitation index in arid locations and dry seasons. *International Journal*
21 *of Climatology*, 27(1), 65–79, 2007.

22 Xie, P., and Arkin, P. A.: Global precipitation: A 17-year monthly analysis based on gauge
23 observations, satellite estimates, and numerical model outputs. *Bull. Amer. Meteor. Soc.*, 78,
24 2539 – 2558, 1997.

25 Zambrano-Bigiarini M.: hydroGOF: Goodness-of-fit functions for comparison of simulated
26 and observed hydrological time series. R package version 0.3-7. [http://CRAN.R-](http://CRAN.R-project.org/package=hydroGOF)
27 [project.org/package=hydroGOF](http://CRAN.R-project.org/package=hydroGOF), 2013.

28

29

1

2 Table 1. Geographical extent of the African regions and number of grid cells analysed for
3 each dataset. For GPCC, the percentage of stations per grid and the percentage of pixels
4 without stations are respectively shown between brackets.

Region	Area (10⁶xKm²)	Longitude-Latitude	GPCC Grid cells
A - Oum er-Rbia	0.49	[10°W-0°E]X[31°N-35°N]	36 (52, 65)
B - Niger	1.48	[10°W-0°E]X[6°N-18°N]	120 (23, 70)
C - Eastern Nile	1.23	[30°E-40°E]X[7°N-17°N]	100 (23, 75)
D -Limpopo	0.94	[25°E-34°E]X[26°S-20°S]	54 (56, 44)
E -GHA	2.22	[40°E-52°E]X[2°S-12°N]	180 (15, 85)

5

6

7

8

1 Table 2. Description of global datasets available in near-real time that could be used for
 2 monitoring precipitation conditions at continental level.

<i>Datasets</i>	<i>resolution</i>	<i>period</i>	<i>Source</i>	<i>Update</i>
ERA INTERIM	0.5°x0.5°	1979-present	ECMWF Reanalysis	½ month
TRMM 3B-43 v.6	0.25°x0.25°	1998-present	Remote Sensing Estimate (combination 3B-42, CAMS and/or GPCC)	1 or 2 months
GPCC v.5	0.5°x0.5°	1901-2010	In-situ data	1 month
GPCP v.2.2	2.5°x2.5°	1979-2010	Remote Sensing Estimate(merged from microwave, infrared and sounder data and precipitation gauge analyses (GPCC).	irregular
CMAP	2.5°x2.5°	1979-2009	Remote Sensing Estimate (GPI, OPI,S SM/I scattering, SSM/I emission and MSU + NCEP/NCAR Reanalysis)	irregular

3
 4
 5

1 Table 3. Correlation coefficient (r), Mean absolute difference (MAD) and percent bias (%)
 2 between the different precipitation datasets averaged over each region for the common period
 3 1998-2010. All correlations are significant at 99%.

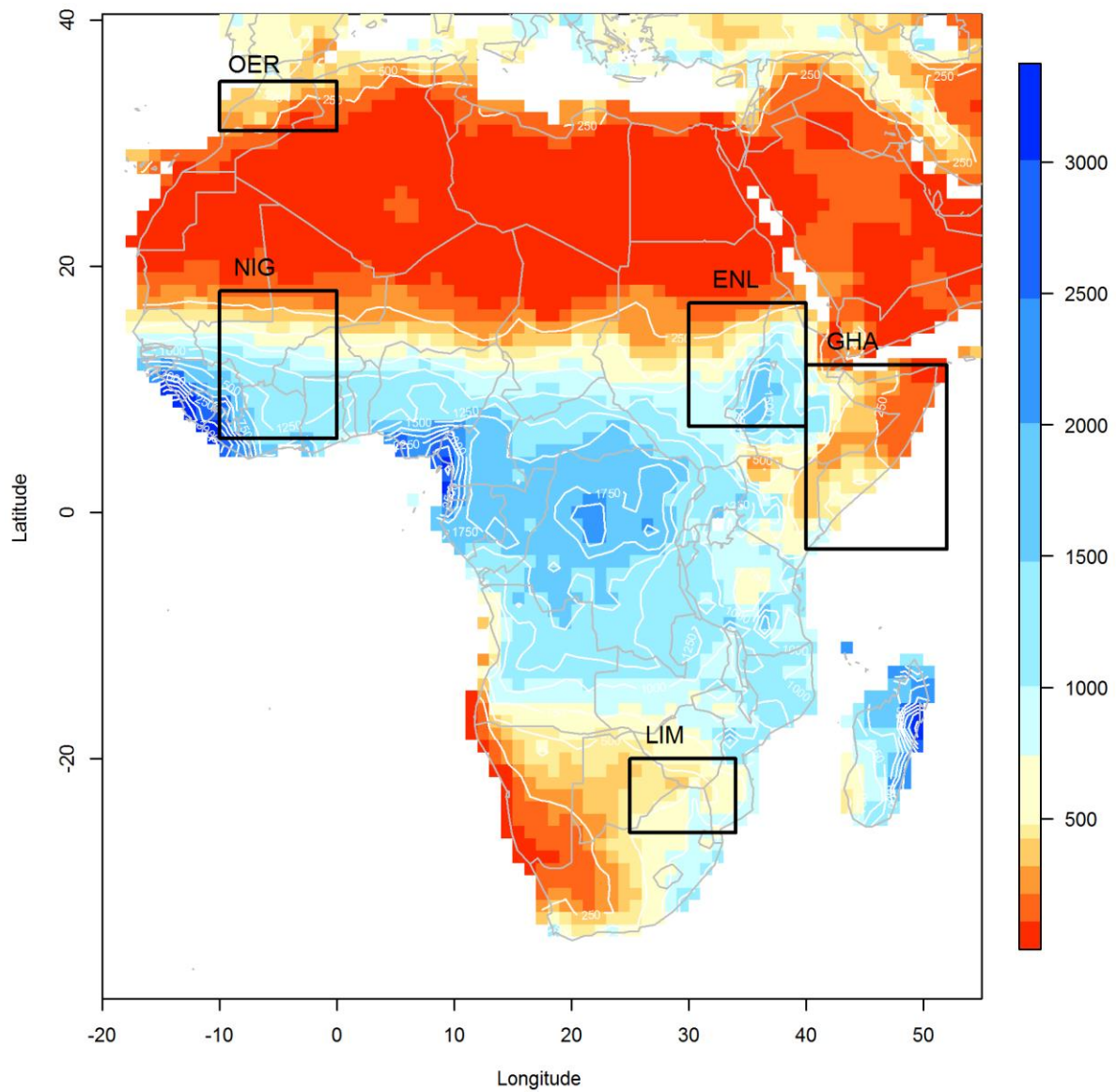
		<i>TRMM</i>			<i>GPCC</i>			<i>GPCP</i>			<i>CMAP</i>			<i>ERA-I</i>		
		r	MAD	BIAS	r	MAD	BIAS	r	MAD	BIAS	r	MAD	BIAS	r	MAD	BIAS
OER	TRMM	-	-	-	0.99	2.5	2.7	0.99	2.9	6.7	0.74	7.8	42.8	0.95	7.3	26.3
	GPCC	0.99	2.5	-2.6	-	-	-	0.99	2.5	4.2	0.94	4.7	23.1	0.95	6.7	24.4
	GPCP	0.99	2.9	-6.2	0.99	2.5	-4	-	-	-	0.73	6.5	33.9	0.95	5.7	18.4
	CMAP	0.74	7.8	-30	0.94	4.6	-18.7	0.73	6.5	-25.3	-	-	-	0.68	7.0	-11.6
	ERA-I	0.95	7.3	-20.8	0.95	6.6	-19.6	0.95	5.7	-15.5	0.68	7.0	13.1	-	-	-
NIG	TRMM	-	-	-	0.99	5.8	-1.9	0.98	13.6	-14.5	0.8	13.9	7.2	0.94	23.2	8
	GPCC	0.99	5.8	1.9	-	-	-	0.99	11.6	-14.1	0.97	6.9	-1	0.95	22.2	8.3
	GPCP	0.98	13.6	17	0.99	11.5	16.4	-	-	-	0.82	16.7	25.4	0.95	25.8	26.4
	CMAP	0.8	13.8	-6.7	0.97	6.9	1	0.82	16.8	-20.3	-	-	-	0.78	25.8	0.7
	ERA-I	0.94	23.1	-7.4	0.95	22.2	-7.7	0.95	25.8	-20.9	0.78	25.8	-0.7	-	-	-
ENL	TRMM	-	-	-	0.94	17.6	-23.7	0.93	17.4	-22.4	0.82	15.3	-0.6	0.93	43.9	-48.1
	GPCC	0.94	17.6	31	-	-	-	1	2.7	1.9	0.97	12.1	22.5	0.97	29.9	-32.3
	GPCP	0.93	17.4	28.9	1	2.66	-1.9	-	-	-	0.85	14.3	28.2	0.97	30.1	-33.1
	CMAP	0.82	15.3	0.6	0.97	12.1	-18.4	0.85	14.3	-22	-	-	-	0.86	43.4	-47.8
	ERA-I	0.93	43.9	92.8	0.97	29.9	47.6	0.97	30.1	49.5	0.86	43.4	91.7	-	-	-
LIM	TRMM	-	-	-	0.98	7.03	8.9	0.97	8.4	6.7	0.76	12.6	20.6	0.96	10.4	9
	GPCC	0.98	7.0	-8.2	-	-	-	0.99	5.1	-3.3	0.91	8.3	1.8	0.98	8.1	-1.5
	GPCP	0.97	8.4	-6.3	0.99	5.1	3.4	-	-	-	0.79	9.9	13	0.97	8.8	2.1
	CMAP	0.76	12.6	-17	0.91	8.3	-1.8	0.79	9.9	-11.5	-	-	-	0.79	12.8	-9.6
	ERA-I	0.96	10.4	-8.2	0.98	8.1	1.5	0.97	8.8	-2.1	0.79	12.8	10.6	-	-	-
GHA	TRMM	-	-	-	0.82	9.8	-4.2	0.88	6.6	1.7	0.72	9.2	11.2	0.84	17.8	-34
	GPCC	0.82	9.8	4.4	-	-	-	0.9	8.2	7.1	0.84	9.4	8.4	0.83	17.1	-30.9
	GPCP	0.88	6.6	-1.7	0.9	8.2	-6.6	-	-	-	0.7	9.6	9.3	0.92	16.4	-35.1
	CMAP	0.72	9.2	-10.1	0.84	9.4	-7.8	0.7	9.6	-8.5	-	-	-	0.61	22.7	-40.6
	ERA-I	0.84	17.8	51.5	0.83	17.1	44.7	0.92	16.4	54.1	0.61	22.7	68.4	-	-	-

4
5
6
7
8
9
10

1 Table 4. Spearman correlation coefficient (r), mean absolute difference (MAD) between the
 2 different SPI-3 estimations averaged over each region for the common period 1998-2010

		<i>TRMM</i>		<i>GPCC</i>		<i>GPCP</i>		<i>ERA-I</i>	
		<i>r</i>	<i>MAD</i>	<i>r</i>	<i>MAD</i>	<i>r</i>	<i>MAD</i>	<i>r</i>	<i>MAD</i>
Oumer-Rbia	TRMM	-	-	0.89	0.28	0.81	0.38	0.84	0.37
	GPCC	0.89	0.28	-	-	0.81	0.35	0.81	0.34
	GPCP	0.81	0.38	0.81	0.35	-	-	0.74	0.5
	ERA-I	0.84	0.37	0.81	0.34	0.74	0.5	-	-
Niger	TRMM	-	-	0.85	0.26	0.79	0.38	0.71	0.5
	GPCC	0.85	0.26	-	-	0.91	0.29	0.72	0.46
	GPCP	0.79	0.38	0.91	0.29	-	-	0.67	0.65
	ERA-I	0.71	0.5	0.72	0.46	0.67	0.65	-	-
Blue Nile	TRMM	-	-	0.54	0.54	0.53	0.55	0.6	0.5
	GPCC	0.54	0.54	-	-	0.92	0.27	0.57	0.41
	GPCP	0.53	0.55	0.92	0.27	-	-	0.67	0.46
	ERA-I	0.6	0.5	0.57	0.41	0.67	0.46	-	-
Limpopo	TRMM	-	-	0.91	0.28	0.84	0.39	0.8	0.46
	GPCC	0.91	0.28	-	-	0.92	0.27	0.91	0.33
	GPCP	0.84	0.39	0.92	0.27	-	-	0.88	0.35
	ERA-I	0.8	0.46	0.91	0.33	0.88	0.35	-	-
GHA	TRMM	-	-	0.58	0.4	0.65	0.44	0.61	0.44
	GPCC	0.58	0.4	-	-	0.86	0.29	0.58	0.42
	GPCP	0.65	0.44	0.86	0.29	-	-	0.68	0.45
	ERA-I	0.61	0.44	0.58	0.42	0.68	0.45	-	-

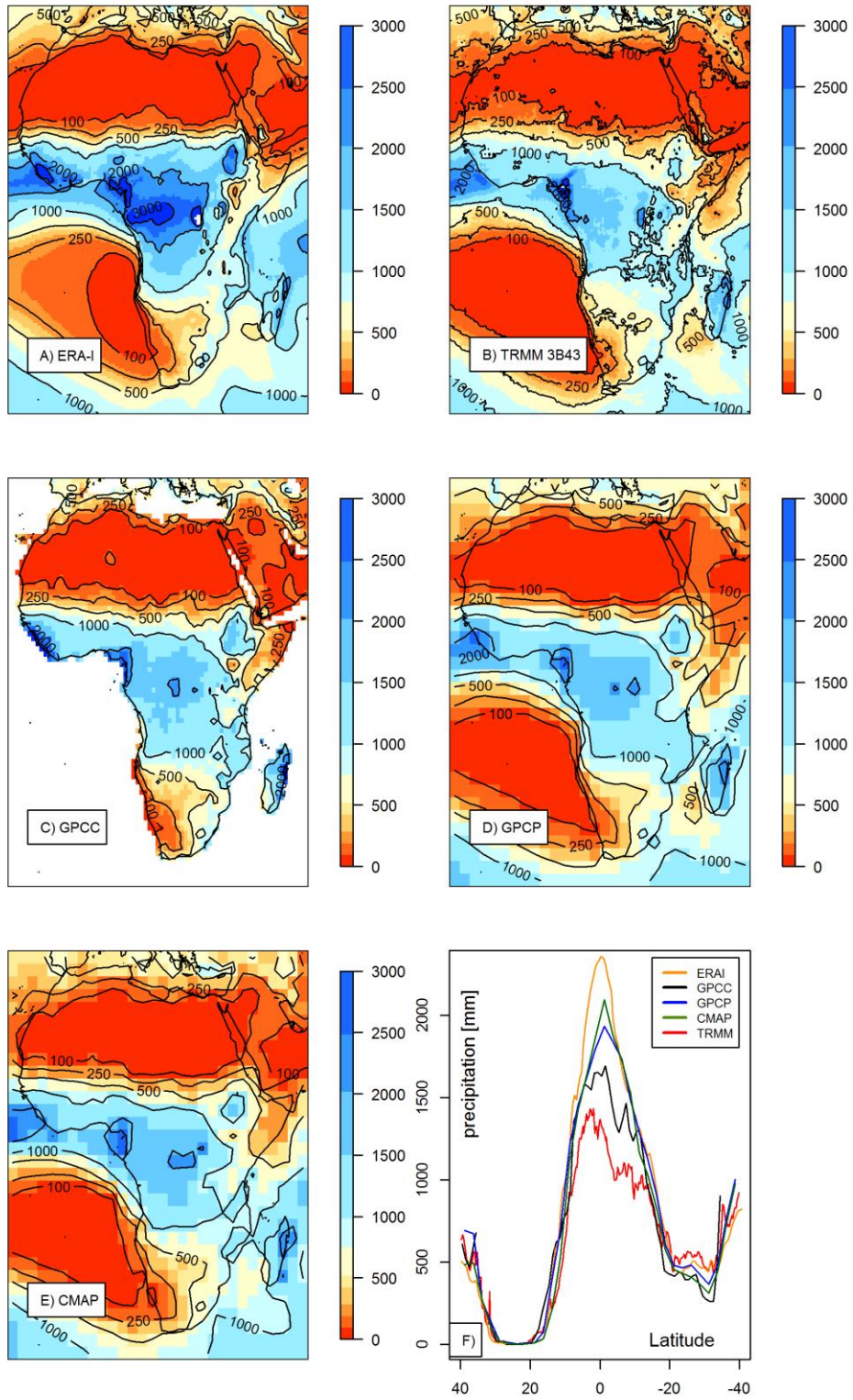
3
 4
 5
 6
 7
 8
 9
 10
 11
 12



1
 2 Figure 1. Annual mean precipitation from the GPCP dataset and African regions used in this
 3 analysis as defined in Table 1. (OER: Oum er-Rbia; NIG: Inner Niger Delta; ENL: Eastern
 4 Nile, LIM: Limpopo basin and GHA: Greater Horn of Africa.

5
 6
 7
 8

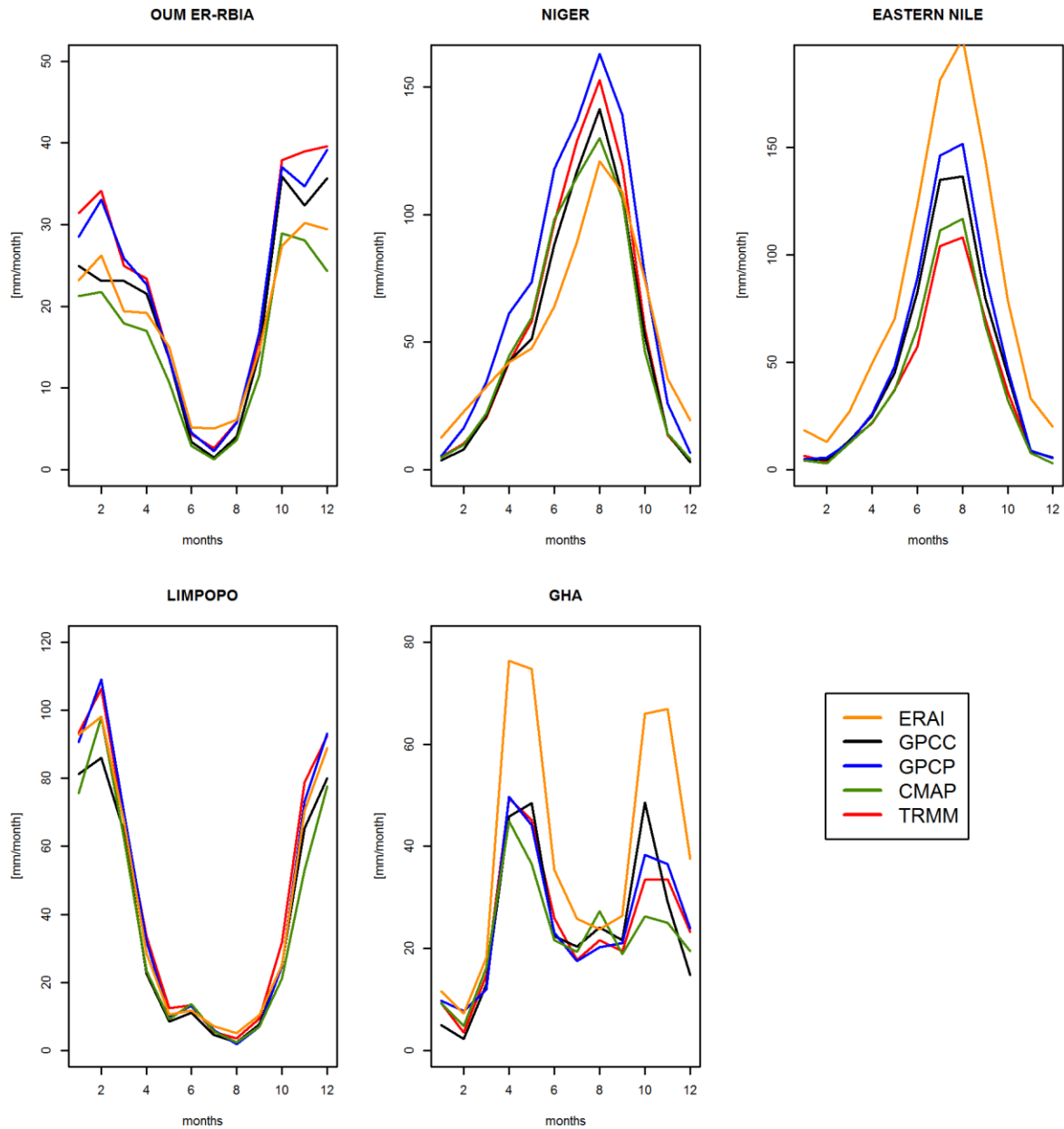
1



2

3 Figure 2. A-E) Mean annual precipitation (mm/year) from different datasets for the common
4 period 1998-2010, F) longitudinal cross section at 25°E of mean annual precipitation.

5



1

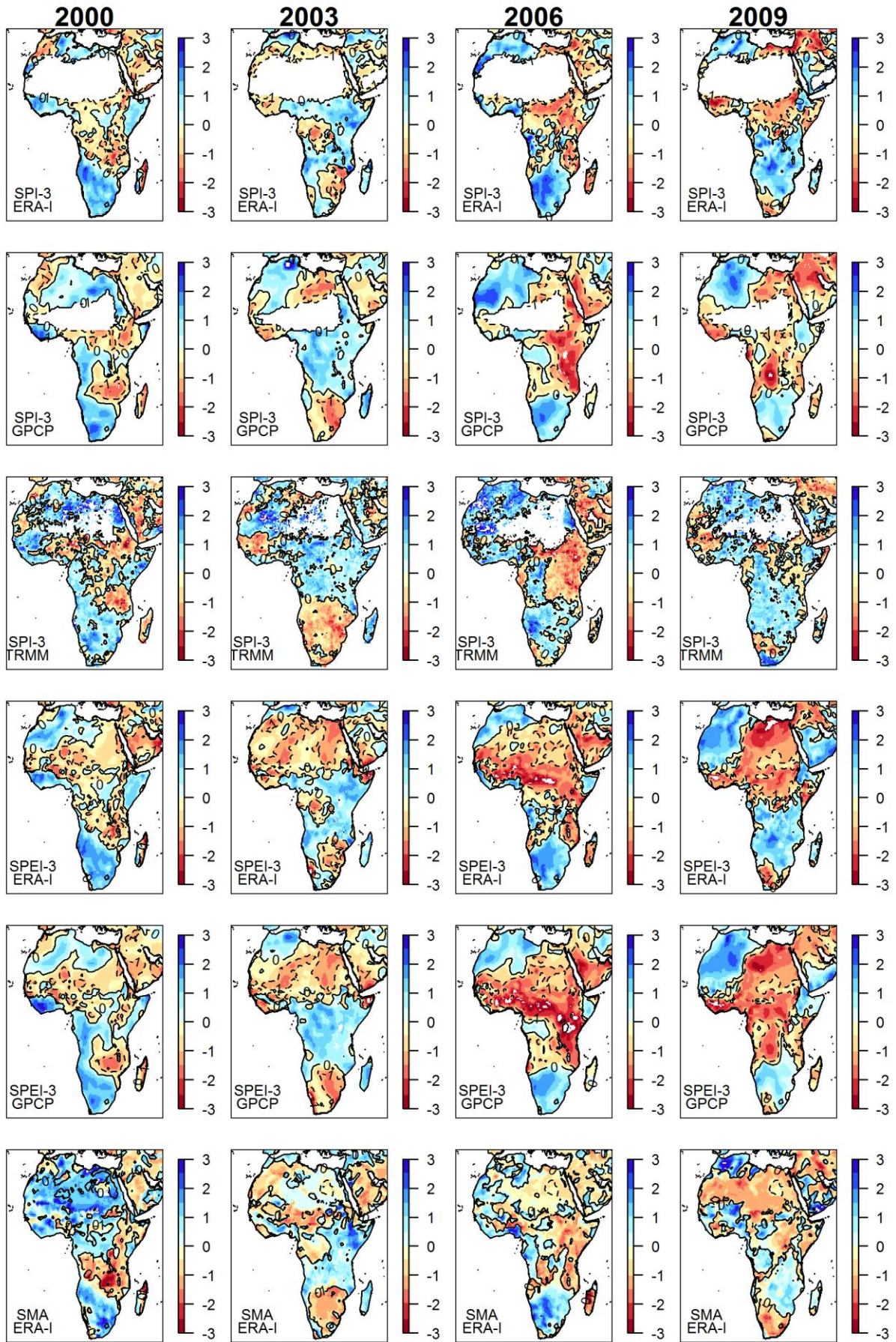
2 Figure 3. Mean annual cycle of precipitation from the different datasets averaged over the five
 3 regions defined in Figure 1 (OER: Oum er-Rbia, NIG: Inner Niger Delta, NIL: Eastern Nile,
 4 LIM: Limpopo basin and GHA: Greater Horn of Africa) for the common period 1998-2010.

5

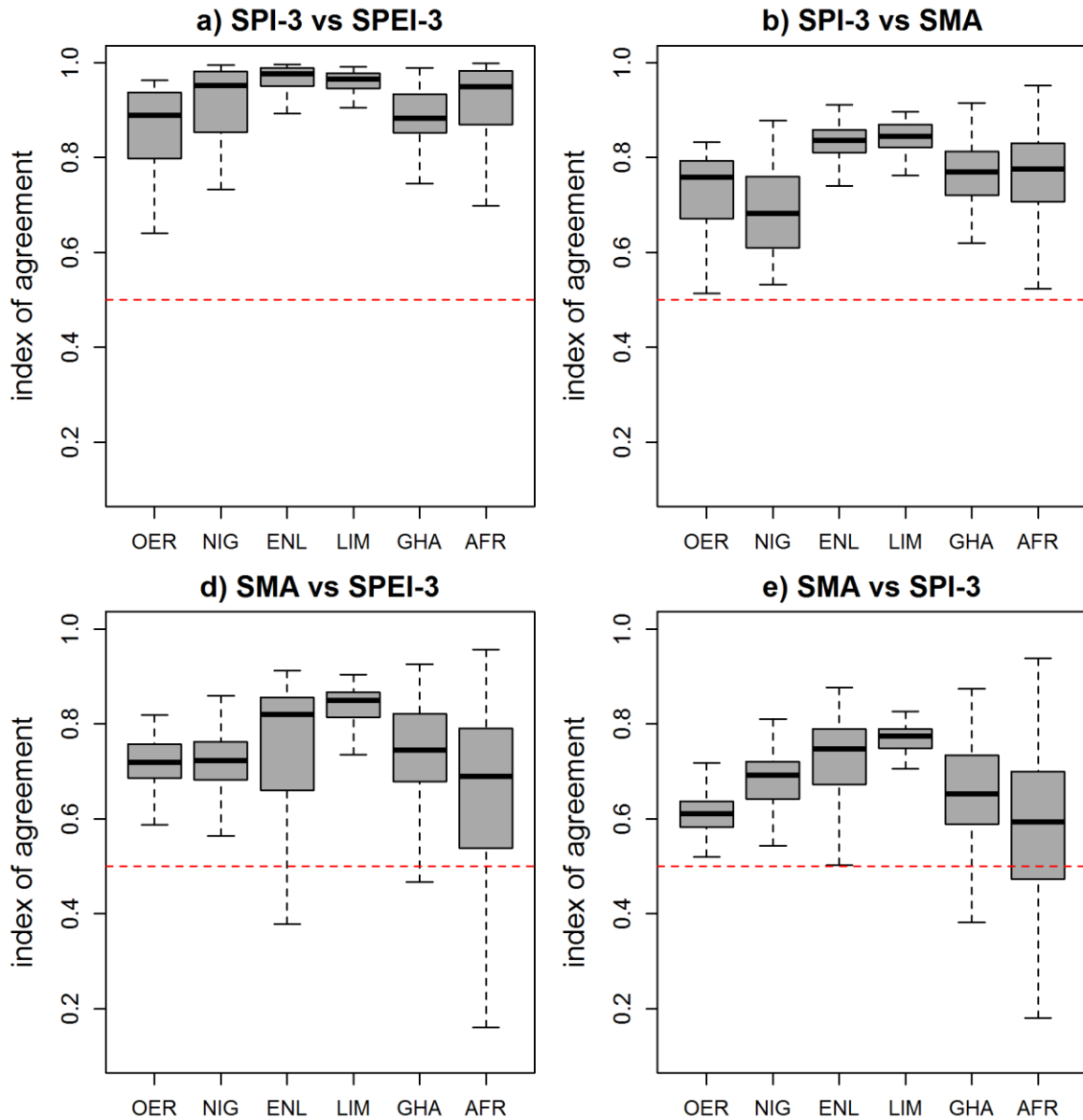
6

7

8



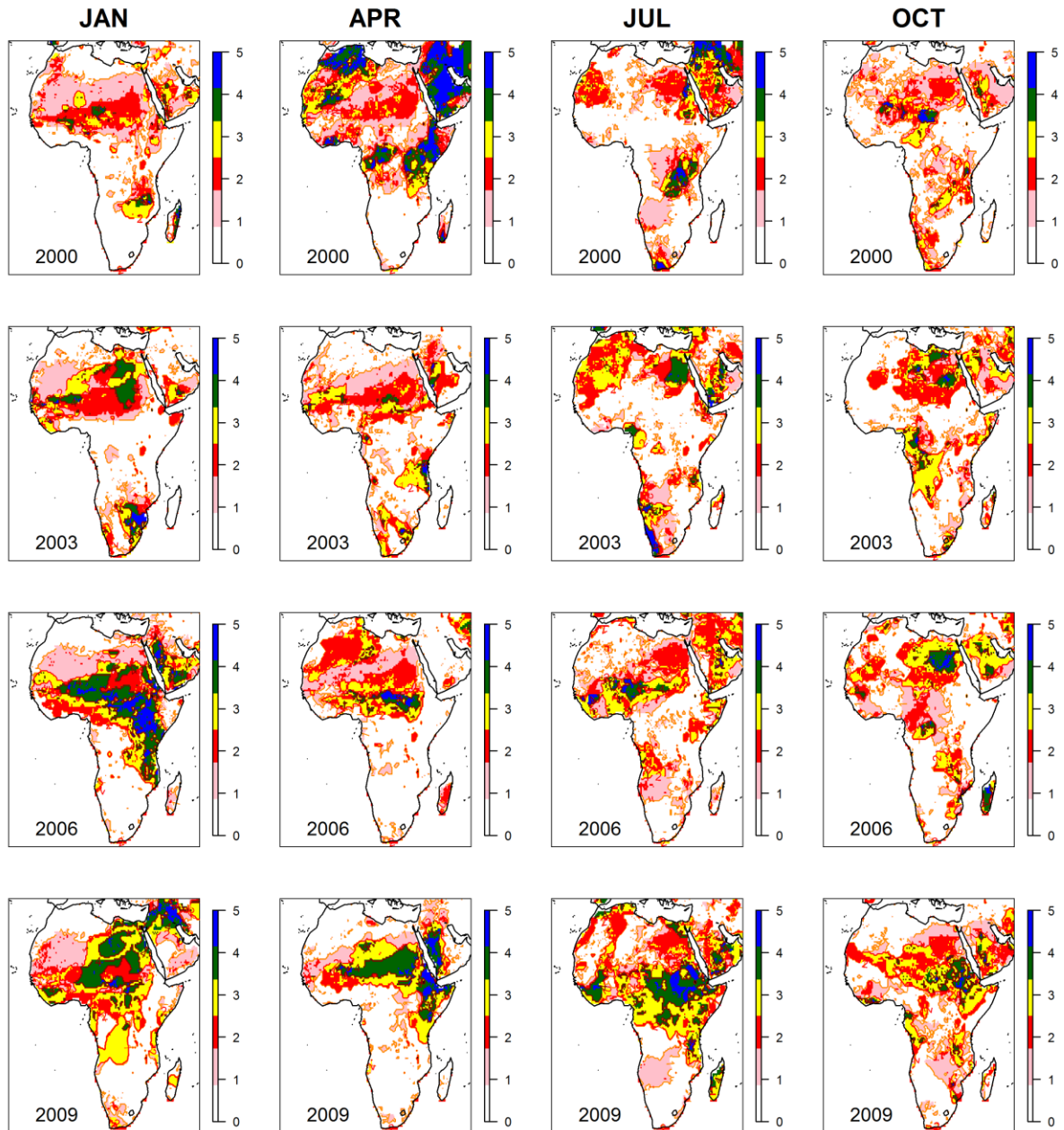
1 Figure 4. Monthly standardized anomalies in SPI-3 (ERA-I, GPCP, TRMM), SPEI (ERA-I
 2 and GPCP) and Soil Moisture (SMA) for January 2000, 2003, 2006 and 2009. Solid lines
 3 indicates the zero contour. White areas represent regions where it was not possible to compute
 4 the gamma parameters for SPI due the large amount of zeros.
 5



6
 7 Figure 5. Index of agreement (d) between SPI, SPEI, ~~and SMA and PET~~-computed using
 8 ERA-I for the five case studies and the whole continent. (OER: Oum er-Rbia, NIG: Inner
 9 Niger Delta, NIL: Eastern Nile, LIM: Limpopo basin and GHA: Greater Horn of Africa).

1 Dashed lines extend from 5th to 95th percentile of estimations, boxes extend from 25th to
2 75th percentile and middle horizontal lines within each box indicate the mean for each region.

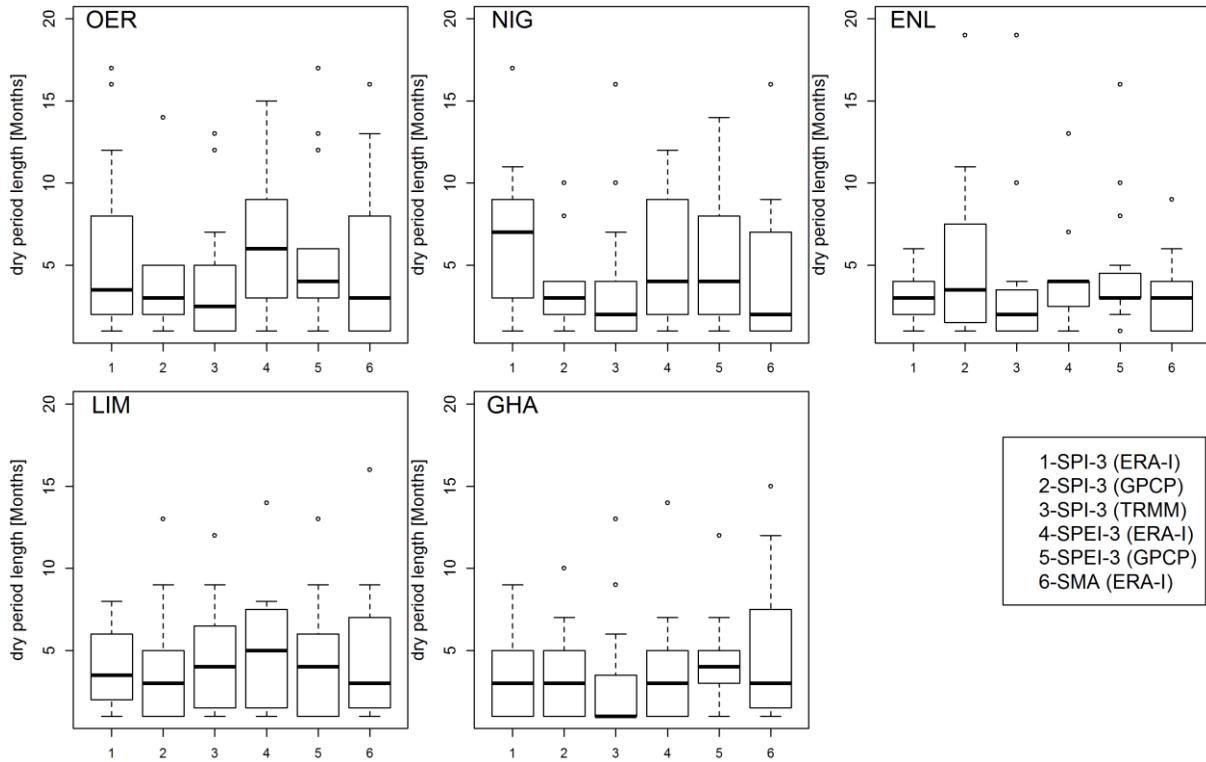
3



4

5 Figure 6. Month by month evolution of droughts in 2000, 2003, 2006 and 2009 according to
6 grid cells with SPI-3/SPEI-3 computed using ERA-I GPCP, and TRMM below -1.0. Values
7 are ranged between 0 (no dataset with SPI-3/SPEI-3 below the threshold) and 5 (all datasets
8 below threshold).

9



2

3 Figure 7. Duration of dry periods for the standardized indicators below zero in the common

4 period 1998-2010. (OER: Oum er-Rbia, NIG: Inner Niger Delta, NIL: Eastern Nile, LIM:

5 Limpopo basin and GHA: Great Horn of Africa). Dashed lines extend from 5th to 95th

6 percentile of estimations, boxes extend from 25th to 75th percentile and middle horizontal

7 lines within each box indicate the mean for each region.

8

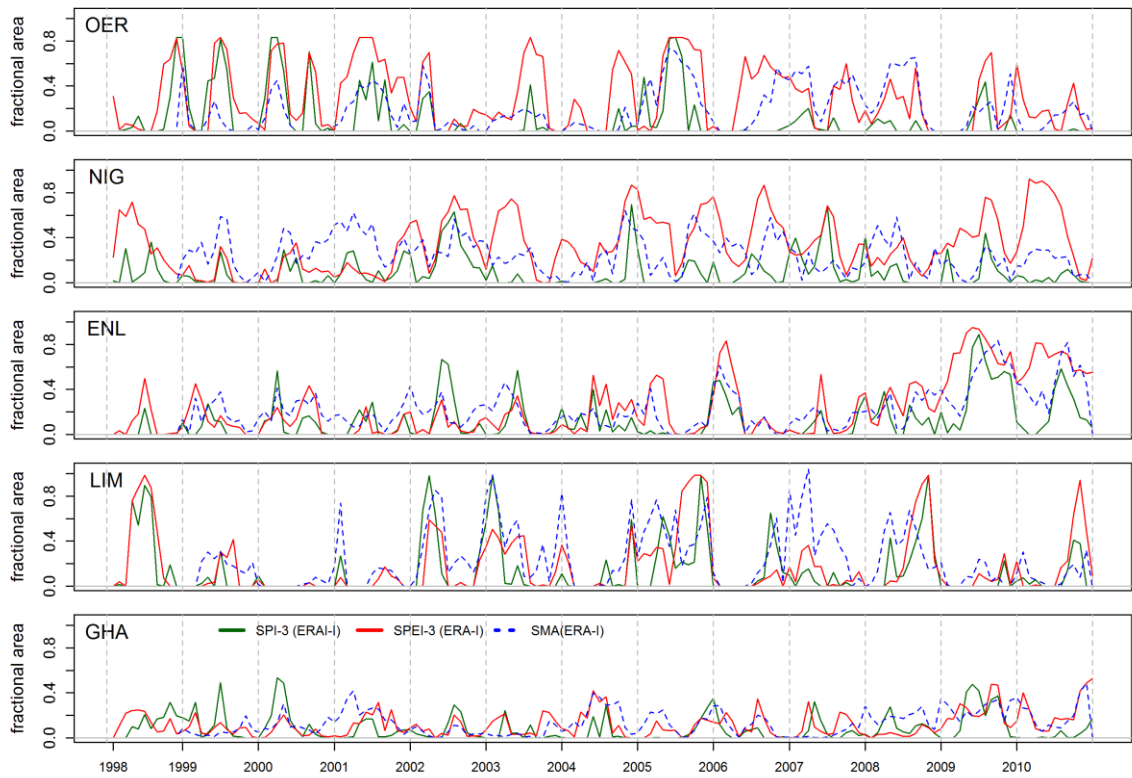
9

10

11

12

13



1

2 Figure 8. Fractional area of each region under SPI, SPEI and SMA ~~and PET z-scores~~ below -
 3 1.0 for the period 1998-2010. (OER: Oum er-Rbia, NIG: Inner Niger Delta, NIL: Eastern
 4 Nile, LIM: Limpopo basin and GHA: Greater Horn of Africa).

5

6

7

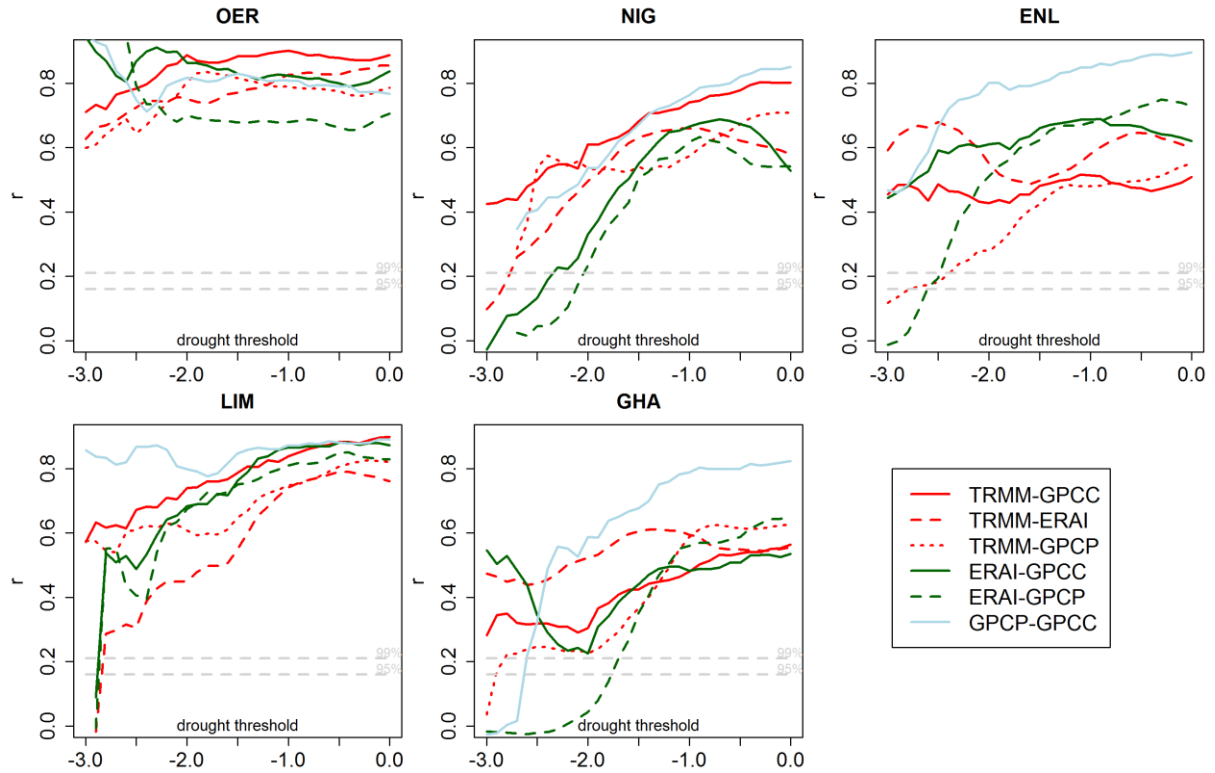
8

9

10

11

12



1

2 Figure 9. Correlation coefficient of fractional areas under drought between different datasets
 3 and thresholds. The horizontal axis represents the SPI threshold below which areas are
 4 considered to be under drought.

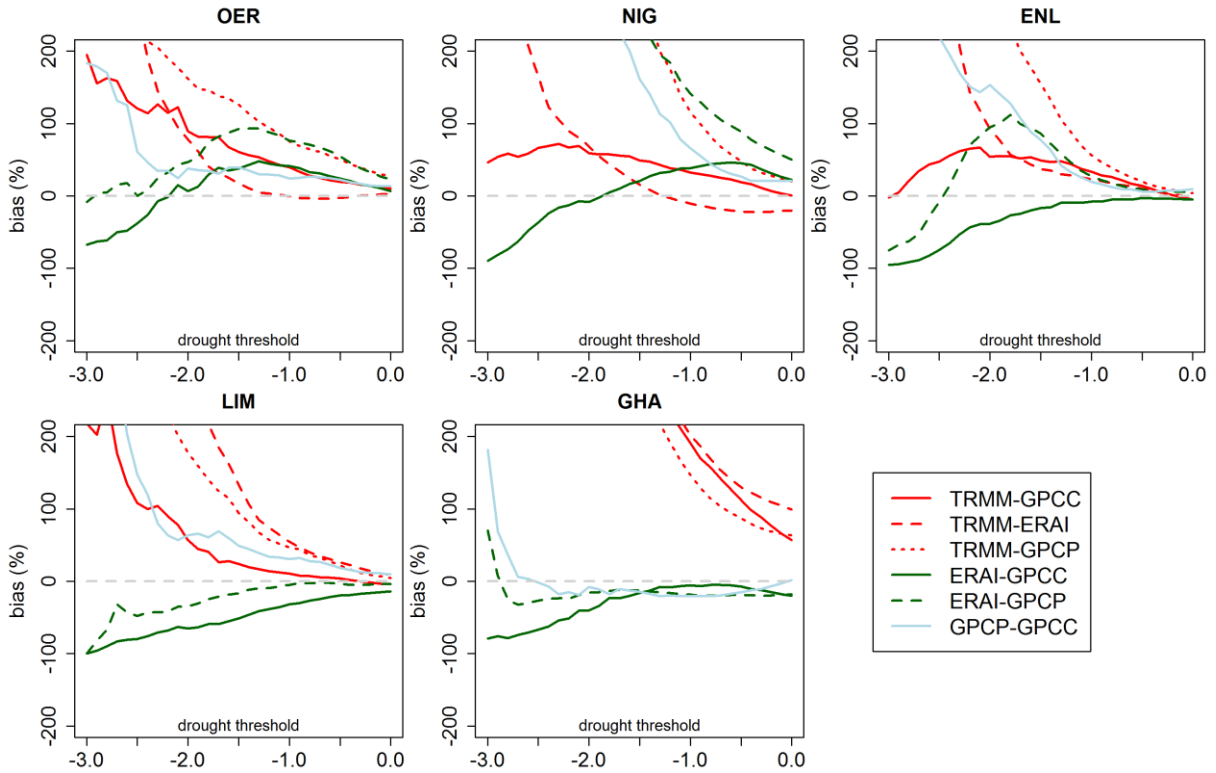
5

6

7

8

9



1

2 Figure 10. Relative bias between the estimation of fractional areas under drought for different
 3 datasets and thresholds. The horizontal axis represents the SPI threshold below which areas
 4 are considered to be under drought.